CORROSION SCIENCE AND TECHNOLOGY, Vol.15, No.5(2016), pp.203~208 pISSN: 1598-6462 / eISSN: 2288-6524
DOI: http://dx.doi.org/10.14773/cst.2016.15.5.203

Study of Hot Salt Stress Corrosion Crack Initiation of Alloy IMI 834 by using DC Potential Drop Method

Mangesh D. Pustode[1,†], Bhupendra Dewangan[2], V. S. Raja[3], Neeta Paulose[4] and Narendra Babu[4]

[1]*Kalyani Centre for Technology and Innovation, Bharat Forge Ltd., Pune 411036, India*

[2]*Research and Development, Tata Steel, Jamshedpur, 831007, India*

[3]*Department of Metallurgical Engineering and Materials Science, Indian Institute of Technology Bombay, Mumbai 400076, India*

[4]*Gas Turbine Research Establishment (GTRE), Bangalore 560093, India*

(Received June 07, 2016; Revised August 29, 2016; Accepted October 20, 2016)

DC potential drop technique was employed during the slow strain rate tests to study the hot salt stress corrosion crack (HSSCC) initiation at 300 and 400 °C. Threshold stresses for HSSCC initiation were found to about 88 % of the yield strength at both temperatures, but the time from crack initiation to final failure (Δt_{scc}) decreased significantly with temperature, which reflects larger tendency for brittle fracture and secondary cracking. The brittle fracture features consisted of transgranular cracking through the primary α grain and discontinuous faceted cracking through the transformed β grains.

Keywords : *titanium, stress corrosion cracking, hydrogen, fractography*

1. Introduction

High specific strength and toughness combined with good corrosion resistance are the key properties of titanium alloys that make them attractive for gas turbine applications, especially in the early stages of the compressor. However, titanium alloys are prone to hot salt stress corrosion cracking (HSSCC) when subjected to stress and salt at elevated temperatures[1-8]. Only a limited literature is available on the HSSCC behaviour of various grades of titanium alloys[2-4,6,9-15], and almost all of them show HSSCC susceptibility. Constant load test (CLT) technique has been widely used to study the HSSCC behaviour of the titanium alloys by several investigators[2,5,7,8,10,13,15-18]. They used different criteria to determine threshold stress (the below which an alloy is considered to be immune to HSSCC) of the same alloy in the same test conditions. Residual mechanical ductility[2,4,13,15,19], stress-rupture life[3,11,16,18], the presence of crack[3,11,16,18] and/or corrosion products are used as criteria to determine of threshold stress for HSSCC. Notably, the residual mechanical ductility approach was the most widely used criterion to evaluate threshold stresses. Since, slow strain rate test (SSRT) is a more rapid technique than CLT; it has been used to determine threshold stresses for several other alloys/environment (ambient temperature) systems[20-24]. To determine the threshold stress by using SSRT, DC potential drop (DCPD) measurement has been employed during test. Threshold stress of an alloy, in these cases, is considered to be equivalent to that stress (in a stress /potential difference diagram) at which the specimen potential begins to deflect from normal trend in DC potential vs. stress plot.

The present study concerns with applying DCPD technique to study alloy IMI 834, that has increased temperature capability and is being employed in the initial stages of the high-pressure compressor components of the aero gas turbine engine. By virtue of its high temperature capability and creep resistance, it has high potential for use in marine gas turbine engine, whose designed life is far more than that of the aero gas turbine engine. Our recent study on the HSSCC susceptibility of alloy IMI 834, using a slow strain rate test (SSRT), has shown that the alloy is susceptible to HSSCC at 300 °C and above[6]. In order to employ this alloy in service, it is important to determine threshold stresses to predict the service life. Hence this study becomes important. The HSSCC study has been carried out at 300 and 400 °C.

†Corresponding author: mdpustode@gmail.com

Table 1. Chemical composition of alloy IMI 834 (wt. %)

Al	Zr	Sn	Nb	Mo	Si	C	Ti
5.97	3.37	3.68	1.31	0.44	0.44	0.078	Bal.

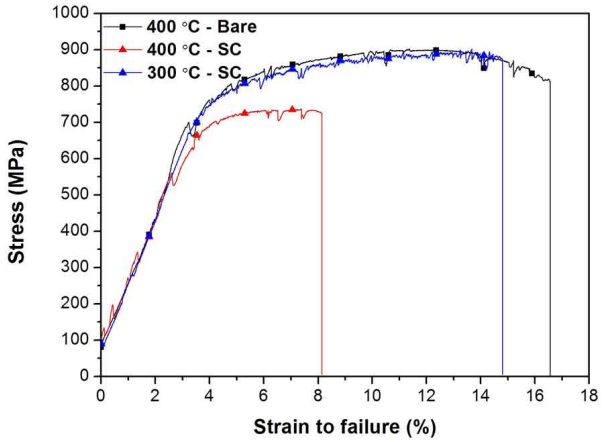

Fig. 1. Apparent stress-strain curves of the specimens tested at a strain rate of 1.6 x 10^{-7} s^{-1} in bare and salt-coated conditions at 400 °C and salt-coated condition at 300 °C. Note: SC represents that the specimen subjected to the SSR test in salt-coated condition.

2. Experimental procedure

The as-received alloy sample was a 45 mm hot-rolled bar in the heat-treated condition. The heat treatment consisted of solutionising at 1022 °C for 2 h and oil quench, followed by aging at 700 °C for 2 h + air cool. The chemical analysis of the IMI 834 alloy was done using inductively couples plasma technique, and the same is given in Table 1.

Cylindrical tensile specimens having 20 mm gage length and 4 mm gage diameter were used for elevated temperature SSRT. Electrical connections to the specimens were provided at outside of the furnace by increasing the shoulder length of the specimens, which was extended beyond the furnace tube. Two pin holes were drilled along each end of the specimen shoulders, and brass dowel were press-fitted in these holes. The gage length of the specimens was degreased prior to salt-coating. A neutral 25 wt. % NaCl salt solution was used for salt-coating. The degreasing and salt-coating have been carried out according to the procedure given by Pustode et al.[6]. A salt coating of 0.4 ± 0.05 mg cm^{-2} weight was achieved in the study.

Bare and salt-coated specimens were subjected to the slow strain rate test at a strain rate of 1.4 x 10^{-7} s^{-1} at 300 and 400 °C. The furnace temperature was maintained ± 1 °C of the set values. Following the procedures described by Atrens et al. and Oehlert et al.[20-24], HSSCC initiation was detected using DCPD method. A direct current of 10 A was applied to the specimen, and potential drop across the specimen was measured using the DC potential drop unit. A reference specimen maintained at the test temperature connected in series with the slow strain rate test specimen to compensate the shift in the specimen resistivity due to temperature variation.

After the test, ultimate tensile strength (*UTS*), elongation (*El*) and reduction in area (*RA*) were measured to examine the effect of salt. The *El* and *RA* were obtained by measuring the final gage length on the failed specimen and the diameter at the fractured location respectively. Gage surfaces of the failed specimens were investigated for the cracks using a stereo microscope, and fractographic analysis was carried out using a scanning electron microscopy (SEM) to analyse the fracture mode.

3. Results and Discussion

3.1 Determination of threshold stress

Apparent stress-strain curves of the specimens tested at a strain rate of 1.6 x 10^{-7} s^{-1} in bare and salt-coated conditions at 400 °C and in salt-coated condition at 300 °C are shown in Fig. 1. Summary of the slow strain rate test data is presented in Table 2. The data does not include 0.2% offset stress (proof stress) as no extensometer was used during the SSRT due to inherent difficulties in mounting the same. The *El* and *RA* values presented in the Table 2 are obtained by measuring the final gage

Table 2. Summary of SSRT results of alloy IMI 834 in bare and salt-coated conditions at a strain rate of 1.6 x 10^{-7} s^{-1}

Environment	*El* (%)	*RA* (%)	*UTS* (MPa)
300 °C, bare	14*	33*	863*
300 °C, salt-coated	7.5	24	868
400 °C, bare	15	35	901
400 °C, salt-coated	5	13	738

*indicate that *El*, *RA* and *UTS* values of the bare IMI 834 alloy specimen tested at 300 °C and at a strain rate of 10^{-6} s^{-1} are taken from the literature for comparison[6].

length on the failed specimen and the diameter at the fractured location respectively. At 300 °C test temperature, specimen tested in the salt-coated condition shows a considerable reduction in ductility in relation to the bare specimen. Thus the alloy showed 7.5% *El* in the salt-coated condition in relation to the 14% *El* in the bare condition, indicating its susceptibility to HSSCC. The extent of loss in ductility was found to increase with an increase of test temperature, indicating the extent of susceptibility increases with increasing the test temperature. These observations are corroborated with our earlier findings on titanium alloys, IMI 834, Ti-6242S and Ti-6Al-4V tested at a strain rate of 1.6 x 10^{-6} s^{-1} [6,25,26].

DC potential vs. stress curves are shown in Fig. 2. Fig. 2a shows DC potential measurements at 400 °C, in bare and salt-coated conditions. An elastic deformation of the material is characterized by a small, constant and positive gradient at the initial part potential curve (Fig. 2a). At higher stress levels, potential curve became significantly nonlinear in both the bare and salt-coated conditions. However, non-linearity in the potential curve was seen at much lower stress in the salt-coated condition in relation to the bare condition. Such difference is due to the susceptibility of the alloy to HSSCC. Non-linearity in potential curve of the bare specimen was attributed to the onset of plastic deformation and the corresponding stress is represented as σ_{PD} (Fig. 2b), which is in agreement with the earlier studies on magnesium alloys[20,22,23]. In the salt-coated condition, non-linearity in the potential curve was attributed to the initiation of hot salt stress corrosion crack and the corresponding stress is represented as threshold stress (σ_{SCC}). The apparent plastic deformation is observed in case that salt-coated specimen is largely attributed to the stress corrosion crack propagation. The crack propagation eventually leads to the reduction in engineering stress and ductility.

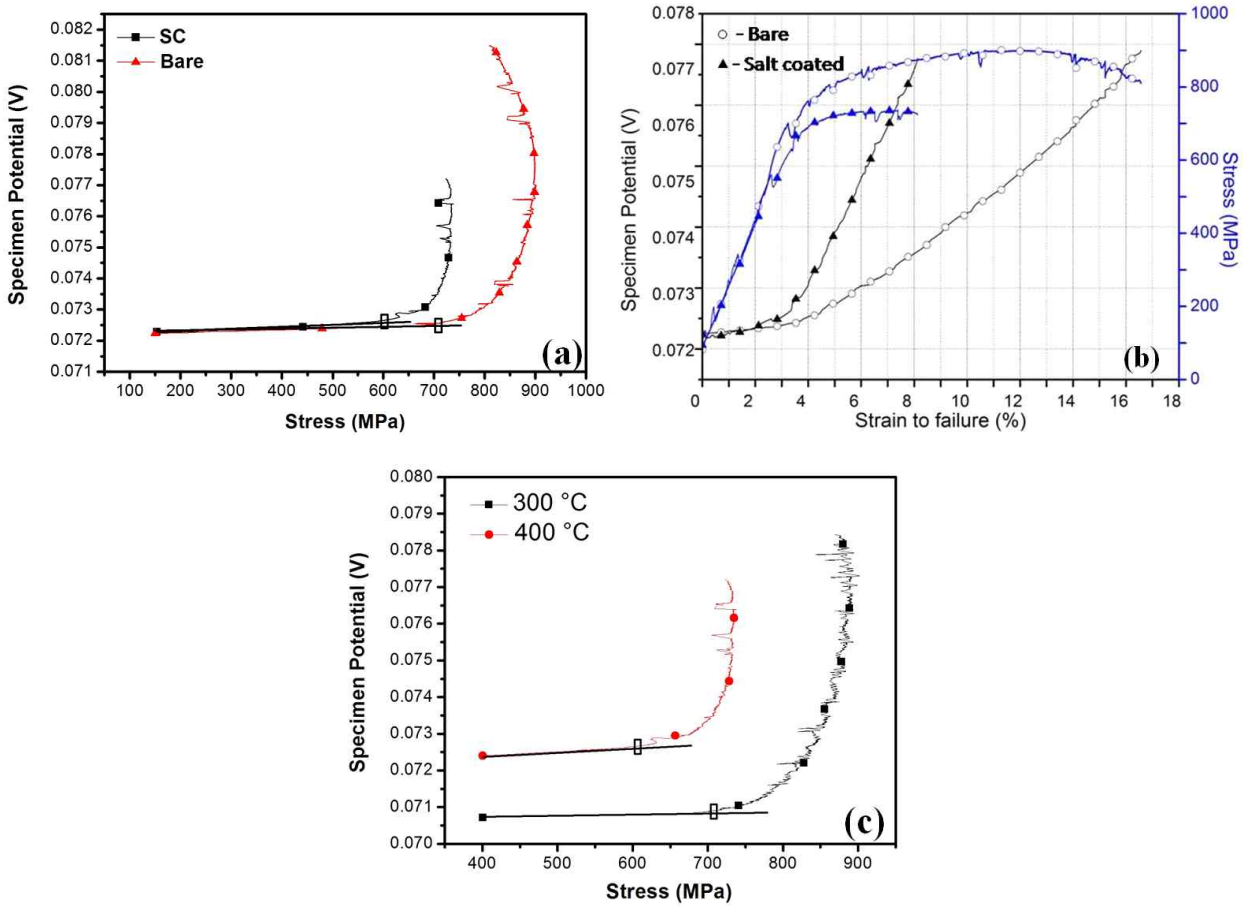

Fig. 2. (a) DC potential vs. stress curves of the alloy IMI 834 tested at 400 °C in bare and salt-coated condition, (b) stress vs. apparent strain and DC potential vs. apparent strain curves for IMI 834 alloy tested at 400 °C in the bare and salt-coated condition and (c) DC potential vs. stress curves of the alloy IMI 834 tested at 300 and 400 °C in salt-coated condition. Note: SC represents specimen tested in salt-coated condition.

Table 3. SCC parameters of the alloy IMI 834 at 300 and 400 °C

Environment	σ_{PD}, σ_{SCC} (MPa)	σy *	σ_{PD},σ_{SCC}/σy*	Δt_{SCC} (h)
400 °C, bare	703	681*	1.03	-
400 °C, salt-coated	602	681*	0.88	100
300 °C, salt-coated	708	795*	0.89	220

*indicate the yield strength values of the alloy IMI 834 in bare condition taken from the literature, having same processing and heat treatment history. σ_{PD} represents threshold stress for the onset of plastic deformation in the bare condition and σ_{SCC} represents threshold for the hot salt stress corrosion crack initiation in salt-coated condition.

The HSSCC parameters derived from DC potential vs. stress curves are summarized in Table 3. For the specimen tested at 400 °C in bare condition, yield strength of the material and the stress where potential become non-linear differ only marginally, supporting our statement that changes in potential pertain to the onset of plastic deformation. At 400 °C, hot salt stress corrosion crack was found to initiate well below the yield strength of the alloy (Table 3). Fig. 2c compares DCPD vs. stress plots of the specimens tested at 300 and 400 °C in the salt-coated conditions. Nonlinearity in the potential curve was seen at much lower stress value at 400 °C test temperature in relation to the specimen tested at 300 °C. Furthermore, it can be said that the hot salt stress corrosion cracks initiate at ~ 88% of the yield strength at both the test temperatures (Table 2).

Earlier studies[22,24] have shown that Δtscc is the time between the crack initiation (furnished by the DC potential drop results) and end of the test. Δt_{scc} values obtained from the DC potential curves of the salt-coated specimens are presented Table 3. The specimens tested at 300 and 400 °C showed Δtscc values of 220 and 100 h respectively. From these results, it can be suggested that, the hot salt stress corrosion cracks grew at higher rate in the specimen tested at 400 °C in relation to the specimen tested at 300 °C.

3.2 Fracture behaviour

The occurrence of hot salt stress corrosion cracking was further confirmed by using surface examination of the failed specimens and fractographic analysis. Stereo-microscopic images of the gage surfaces and the fractographs of the specimens tested at 300, and 400 °C are shown in Fig. 3. Figs. 3a and b show the stereo-microscopic image of the gage surface and fractograph respectively of specimen tested at 400 °C in the bare condition. The stereomicroscopic image of the specimen tested in the bare condition does not reveal any cracks at this magnification on the gage surface (Fig. 3a) and the fracture features showed the presence of dimples indicating ductile failure of the specimen.

The specimen tested in salt-coated condition at 300 °C revealed a few secondary cracks on the gage surface of the failed specimen (Fig. 3c), they become more distinct and large in number when the test temperature was raised to 400 °C (Fig. 3e).These cracks are perpendicular to the loading direction. This is in contrast to the behaviour of the specimen, tested in bare condition, where the stereomicroscope could not reveal their presence. The appearance of such secondary cracks was reported in our earlier studies on the slow strain rate tested specimens of IMI 834 and Ti-6Al-4V alloys[6,26]. It was suggested that the presence of secondary cracks was an indication of hot salt stress corrosion cracking and the depth and the number of the cracks represents the extent to which the alloy is susceptible to SCC.

In contrast to the bare specimen, fractographs of the specimens tested at 300 and 400 °C in salt-coated condition revealed the presence of the brittle fracture features near the edge region (Figs. 3d and f). The fracture features consisted of transgranular cracking of the primary α grains and discontinuous faceted cracking through the transformed β regions of the alloy (Figs. 3d and f). Evidence of secondary cracking and the presence of the brittle fracture feature confirm the occurrence of hot salt stress corrosion cracking and validate threshold stress calculations. Further, the depth of brittle crack was found to be ~120 μm at 300 °C and ~300 μm at 400 °C. Oehlert at al.[20] and Winzer et al.[22,23] have studied the crack initiation on cylindrical specimens using DCPD measurement and calculated the stress corrosion crack velocity (Vc) by measuring brittle crack length on the fracture surface and Δtscc. However, author's suggestion that the crack velocity calculation based on DCPD data is erroneous, due to the occurrence of several secondary cracks on the gage surface of cylindrical tensile specimens during HSSCC.

Several studies have reported that the hydrogen generated during the electrochemical reactions between titanium alloys and salt at elevated temperature, as given below, is responsible for HSSCC [2-5,7,16,27].

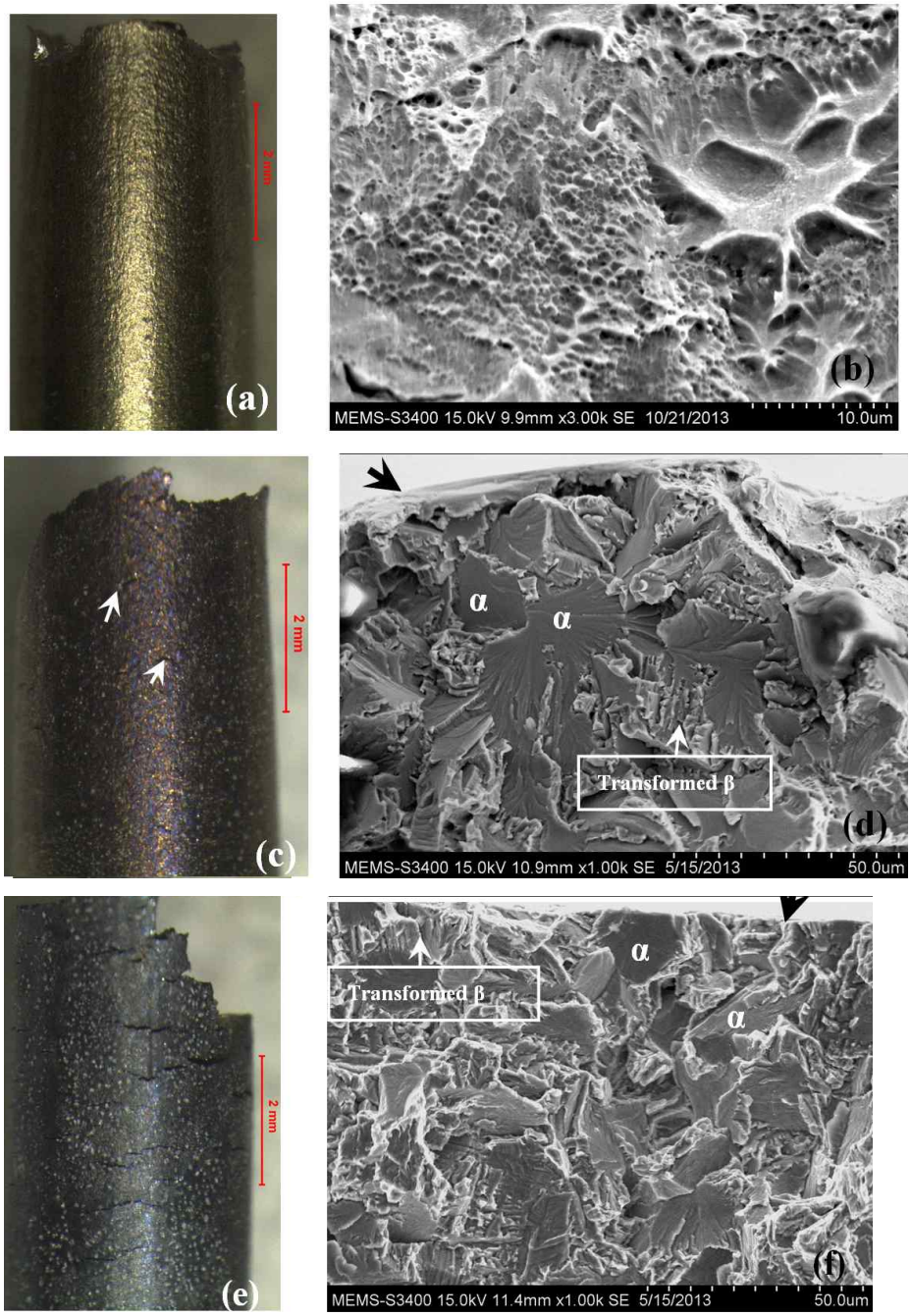

Fig. 3. Stereomicroscopic images of the gage surfaces and the fractographs of the specimens failed in SSRT at: (a) and (b) 400 °C, without salt-coating showing absence of cracks on the gage surface and dimple features respectively, (c) and (d) 300 °C, with salt-coating showing few secondary cracks on gage surface and faceted fracture features respectively, (e) and (f) 400 °C, with salt-coating showing several secondary cracks on gage surface and faceted fracture features respectively.

$$TiO_{2(s)} + 2NaCl_{(s)} + H_2O_{(g)} \xrightarrow{T} Na_2TiO_{3(s)} + 2HCl_{(g)} \quad (1)$$

$$M_{(S)} + xHCl_{(g)} \rightarrow MCl_{x\,(s)} + xH \quad (2)$$

where, M corresponds to Ti, Al and Sn.

At elevated temperature, NaCl salt is likely to react with rutile in presence of water vapour to produce sodium-titanate and hydrochloric acid gas as shown in equation (1). The water needed for this reaction could come from the fluid inclusion retained in the salt or from the adsorbed moisture. The gaseous hydrochloric acid generated above

reacts with the constituent of the alloy according to the generalised reaction[6]. The hydrogen generated by the above reaction diffuses in an alloy to cause embrittlement. The generated hydrogen is expected to bring down the yield strength, as shown by stress vs. DCPD plots, through several mechanisms[28] and in the case of Ti-alloys it would be predominantly through hydride formation. A temperature raise is expected to increase the above reaction kinetics and there by the generation of hydrogen at the specimen surface. Increase in HSSCC in terms of low threshold stress and higher embrittlement at 400 °C in comparison with 300 °C, might therefore be attributed to higher hydrogen evolution kinetics.

4. Conclusions

Threshold stresses for HSSCC of IMI 834 are about 88% of its yield strength at 300 and 400 °C, the test temperatures. As compared to the normal SSR test, where transition from elastic to plastic deformation could not be determined due to non usability of extensometers, DCPD interfaced test provides this information in a much better manner.

Δt_{SCC} values seem to be related to the degree of the susceptibility of the alloy to HSSCC, though it cannot be used to measure crack growth rate, due to the formation of secondary cracks.

Fractographic analysis revealed brittle fracture, and the mechanism of crack growth being transgranular in primary α grains and discontinuous faceted cracking in the transformed β regions.

Acknowledgments

The authors acknowledge the financial support received from the ER-IPR, DRDO, Government of India. Gas Turbine Research Establishment, Bangalore provided the materials.

References

1. T. Chevrot, *Ph. D. Thesis*, Cranfield University (1994).
2. R. K. Dinnappa, *Key Eng. Mat.*, **20-28**, 2255 (1988).
3. NASA TN D-6498, H. R. Gary, Relative Susceptibility of Titanium Alloys to Hot Salt Stress Corrosion (1971).
4. J. D. Jackson, W. K. Boyd, The stress-corrosion and accelerated crack-propagation behaviour of titanium and titanium alloys, DMIC Technical Note, February 1(1966).
5. J. R. Myers, J. A. Hall, *Corrosion*, **33**, 252 (1977).
6. M. D. Pustode, V. S. Raja, N. Paulose, *Corros. Sci.*, **82**, 191 (2014).
7. ASTM STP 397, S. P. Rideout, M. R. Louthan, J. C. L. Selby, Basic mechanisms of stress-corrosion cracking of titanium, p. 137 (1965).
8. G. Sinigaglia, D. Taccani, B. Vicentini, *Corros. Sci.*, **18**, 781 (1978).
9. ASTM STP 397, D. E. Piper, D. N. Fager, The Relative Stress Corrosion Cracking Susceptibility of Titanium Alloys in Presence of Hot Salt, p. 31 (1966).
10. M. Encrenaz, P. Faure, J. A. Petit, *Corros. Sci.*, **40**, 939 (1998).
11. H. R. Gray, J. R. Johnston, Hot-Salt Stress-Corrosion of a Titanium Alloy in a Dynamic Air Environment, *Metall. Trans. A*, **1**, 3105 (1970).
12. R. L. Kirchner, E. J. Ripling, *NASA First Interm Report N65-82069* (1964).
13. M. W. Mahoney, A. S. Tetelman, *Metall. Trans.*, **7**, 1549 (1976).
14. R. S. Ondrejcin, *Metall. Trans.*, **1**, 3031 (1970).
15. ASTM STP 397, R. V. Turley, C. H. Avery, Elevated Temperature Static and Dynamic Sea-Salt Stress Cracking of Titanium Alloys, p. 1 (1966).
16. NASA TN D-5000, H. R. Gray, Hot Salt Stress Corrosion Cracking of Titanium Alloys: Generation of Hydrogen and its Embrittling Effect (1969).
17. NASA TN D-551O, H. R. Gray, J. R. Johnston, Hot-Salt Stress-Corrosion of a Titanium Alloy Under a Simulated Turbine Engine Compressor Environment (1969).
18. NASA TN D-6188, H. R. Gray, Role of Hydrogen in Hot-salt Stress Corrosion of a Titanium Alloy (1971).
19. ASTM STP 397, V. C. Petersen, H. B. Bomberger, The Mechanism of Salt Attack on Titanium Alloys, p. 80 (1966).
20. A. Oehlert, A. Atrens, *Corros. Sci.*, **38**, 1159 (1996).
21. A. Oehlert, A. Atrens, *J. Mater. Sci.*, **33**, 775 (1998).
22. N. Winzer, A. Atrens, W. Dietzel, V. S. Raja, G. Song, K. U. Kainer, *Mater. Sci. Eng. A-Struct.*, **488**, 339 (2008).
23. N. Winzer, A. Atrens, W. Dietzel, G. Song, K. U. Kainer, *JOM-J. Min. Met. Mat. S.*, **59**, 49 (2007).
24. N. Winzer, A. Atrens, W. Dietzel, G. Song, K. U. Kainer, *Mater. Sci. Eng. A-Struct.*, **472**, 97 (2008).
25. M. D. Pustode, V. S. Raja, *Metall. Trans. A*, **46**, 6081 (2015).
26. M. D. Pustode, V. S. Raja, M. Tamilselvi, *Proceedings of the Corrosion 2013 on The stress corrosion cracking susceptibility of Ti-6Al-4V alloy in presence of hot salt*, C2013-2157, Orlando, USA (2013).
27. NASA CR-1133, R. S. Ondrejcin, M. R. Louthan, Role of Hydrogen Chloride in Hot-Salt Stress-Corrosion Cracking of Titanium-Aluminium Alloys (1968).
28. D. F. Teter, I. M. Robertson, H. K. Birnbaum, *Acta Mater.*, **49**, 4313 (2001).